Energies **2011**, *4*, 2180-2195; doi:10.3390/en4122180

OPEN ACCESS

energies

ISSN 1996-1073

www.mdpi.com/journal/energies

Article

Comparison of Extremum-Seeking Control Techniques for Maximum Power Point Tracking in Photovoltaic Systems

Her-Terng Yau * and Chen-Han Wu

Department of Electrical Engineering, National Chin-Yi University of Technology, Taichung 41170, Taiwan; E-Mail: wu.chese@gmail.com

* Author to whom correspondence should be addressed; E-Mail: htyau@ncut.edu.tw; Tel.: +886-4-23924505-7229; Fax: +886-4-23924419.

Received: 8 October 2011; in revised form: 22 November 2011 / Accepted: 6 December 2011 / Published: 8 December 2011

Abstract: Due to Japan's recent nuclear crisis and petroleum price hikes, the search for renewable energy sources has become an issue of immediate concern. A promising candidate attracting much global attention is solar energy, as it is green and also inexhaustible. A maximum power point tracking (MPPT) controller is employed in such a way that the output power provided by a photovoltaic (PV) system is boosted to its maximum level. However, in the context of abrupt changes in irradiance, conventional MPPT controller approaches suffer from insufficient robustness against ambient variation, inferior transient response and a loss of output power as a consequence of the long duration required of tracking procedures. Accordingly, in this work the maximum power point tracking is carried out successfully using a sliding mode extremum-seeking control (SMESC) method, and the tracking performances of three controllers are compared by simulations, that is, an extremum-seeking controller, a sinusoidal extremum-seeking controller and a sliding mode extremum-seeking controller. Being able to track the maximum power point promptly in the case of an abrupt change in irradiance, the SMESC approach is proven by simulations to be superior in terms of system dynamic and steady state responses, and an excellent robustness along with system stability is demonstrated as well.

Keywords: photovoltaic; MPPT; extremum-seeking control; sliding mode control

---

1. Introduction

As a consequence of the global energy crisis and environmental concerns, applications of photovoltaic (PV) systems can be widely found, but they suffer from system inefficiency problems attributed to a number of factors such as the irradiance, the temperature, *etc*., which can be seen from characteristic power *versus* voltage and current *versus* voltage curves. Accordingly, there have been a great number of publications proposing to address such power inefficiency issues [1]. In most cases, solar cells are not operated at the maximum power point due to the load characteristics of a solar cell, a problem that can be resolved via a maximum power point tracking (MPPT) approach. A number of currently employed MPPT approaches [2–6] can be described as follows. Approach 1, the perturbation and observation method (P&O), is a method perturbing the cell load so as to vary the operating point toward the MPP. A resulting disadvantage is the oscillation in the vicinity of MPP, resulting in a power loss and a degraded solar energy conversion efficiency. Approach 2, the incremental conductance method, is a method that intends to locate the maximum power operating point such that the condition $dP/dV = 0$ is satisfied. A major drawback in practical applications is that an error while locating the MPP is inevitably encountered as a consequence of the low precision sensors used. Approach 3, the gradient method, is a relatively complicated control method that evaluates the gradient by numerics, due to which output power fluctuation is seen in under varying ambient conditions. Approach 4, the approximate straight line method, is a method where the P-I characteristic curve is modeled by a piecewise approximation. However, the requirement on this approach is that the cell parameters have to be determined precisely, or otherwise the P-I characteristic curve in the neighborhood of MPP cannot be approximated as a straight line as a consequence of such factors as aging or contaminated solar panels. Approach 5, the voltage feedback method, is a low cost method, but the price paid is that the MPP cannot be tracked in the context of abrupt atmospheric changes. Analogous and relatively complicated in comparison with approach 5, approach 6, the power feedback method, is a method that feeds back the output power rather than the output voltage. In an attempt to eliminate all the above mentioned disadvantages and assure a stabilized system, a sliding mode extremum-seeking control (SMESC) approach is presented in this work to achieve the goal of the MPP tracking.

The extremum-seeking control (ESC) [7] approach is a theory building a feedback system in such a way that oscillation around the MPP is invoked to boost the photovoltaic system efficiency. An alternative ESC approach is to introduce a small amount of perturbation into the control system, according to which a system output response function is then determined to locate the MPP. In this paper, a maximum power tracking controller SMESC is designed in an attempt to improve the system stability and robustness. Relative to the P&Q method, it demonstrates a superior overall efficiency [8] and well maintained robustness in the rapidly varying atmospheric context.

2. Solar Cell Characteristics

As illustrated in Figure 1, a solar cell is a device converting solar energy into electricity and electrons are produced directly by a voltage drop across the PN junction, not by way of an electrolyte.

Figure 1. The working principle of a solar cell [1].

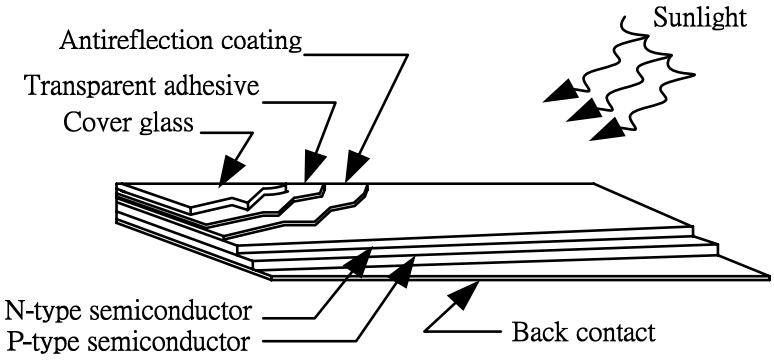

As illustrated in Figure 2, an equivalent circuit of a solar cell is composed of a current source I_{ph}, a diode, an equivalent shunt resistor (R_{sh}) and an equivalent series resistor (R_s) with the output current (I) given as Equation (1):

$$\mathrm{I} = \mathrm{I}_{\mathrm{ph}} - I_{sat}[\exp(\frac{qV_{pv}}{ABT}) - 1] - \frac{(V_{pv} + IR_s)}{R_{sh}} \quad (1)$$

where V_{PV} represents the solar cell output voltage, I_{ph} the output current, I_d the diode current, I_{sat} the photo current at specified irradiance and temperature, A the idea parameter, B the Boltzmann constant, T the reference temperature of the solar cell, q an electron charge, R_s the equivalent series resistor and R_{sh} the shunt resistor caused due to a flawed PN junction.

Figure 2. The equivalent circuit of a solar cell.

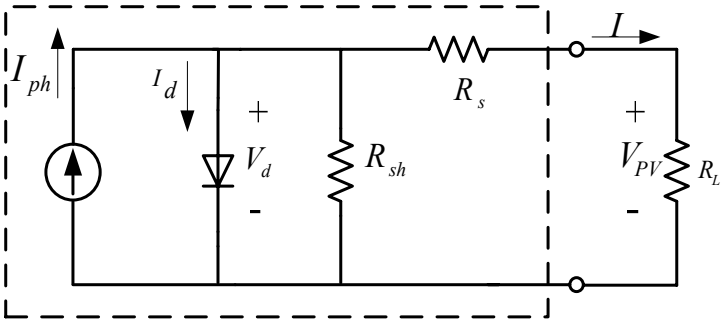

Characteristics of a solar cell, a nonlinear device, are found as functions of solar irradiance. Presented in Figure 3 are I-V characteristic curves of a solar cell loaded with a resistor under standard test conditions.

Figure 3. V-I and P-V characteristic curves of a solar cell.

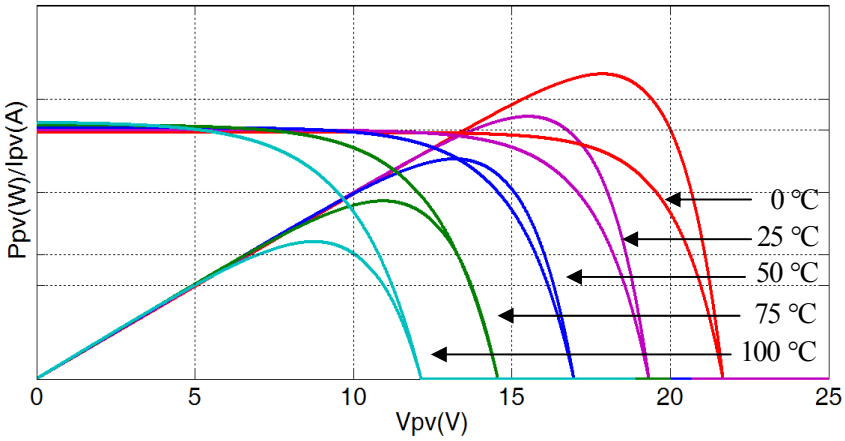

Other than the ambient temperature and solar irradiance, as mentioned previously, the V-I characteristic curve is a nonlinear function of the cell itself and the way it is configured. Accordingly, in practical applications, the maximum power point is a variant position affected by ambience conditions. In an attempt to reach the goal of the MPP tracking, as illustrated in Figure 4, a switched mode power converter lies between the load and the PV array as a way to provide the maximum power at any time.

Figure 4. A block diagram of a PV control system.

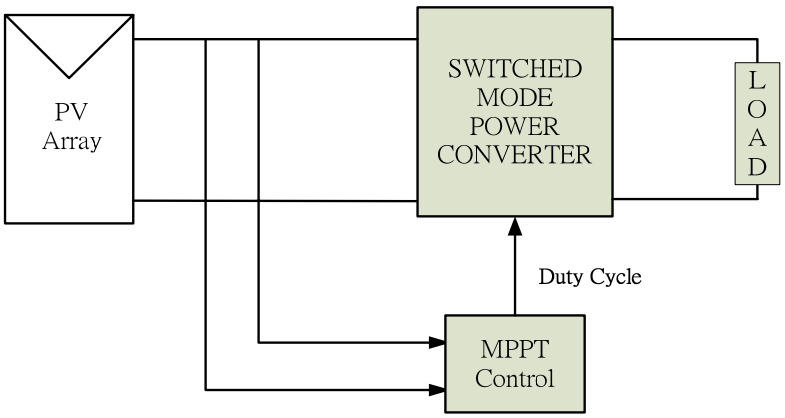

3. Extremum Seeking Control (ESC) Principle

Developed in the 20th century, the ESC [9] is an adaptive control approach that reaches the control target via filtered and driving signals with uncertain or unknown information in some aspects. A major advantage of ESC is that it does not require a system model, and is capable of improving the system performance. Applications of ESC might be found in nonlinear control issues, and nonlinear local minimum and maximum localizations. There might exist local extremums for a nonlinear output P-V characteristic curve in the case of a shaded solar cell.

As illustrated in Figure 5, a system block diagram is composed of an integrator, a differentiator, a logic circuit and an amplifier. ESC is then applied to track the MPP, that is, to located the maximum power point on a *y versus x* curve and overcome the local maximum problem. It is derived from Figure 5 that:

$$\frac{dx}{dt} = K\varepsilon \tag{2}$$

where $\varepsilon = \pm 1$ and K is a positive constant:

$$g = \frac{dy}{dt} \tag{3}$$

In the case $g < 0$, then the signal ε is modified, while it remains unchanged for $g < 0$. The ESC system in Figure 5 is represented by the above equation, and the logic circuit is used to determine whether there is a need to alter ε.

Figure 5. A block diagram of an ESC control system.

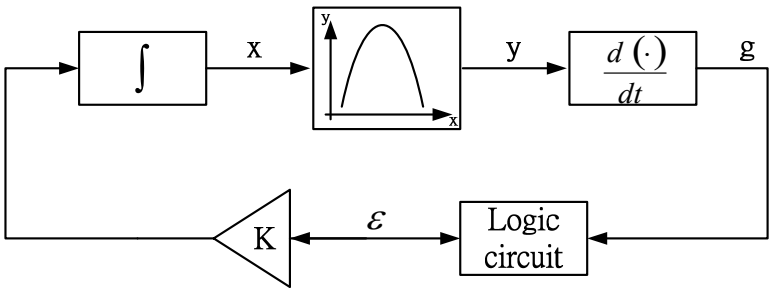

Marked in Figure 6 are the variations [10] in $\frac{dx}{dt}$ and $\frac{dy}{dt}$ of the four points a, b, c, d:

$$a: (\frac{dx}{dt})\Big|_{t=t^-} > 0, (\frac{dy}{dt})\Big|_{t=t^-} > 0 \Rightarrow (\frac{dx}{dt})\Big|_{t=t^+} = k$$

$$b: (\frac{dx}{dt})\Big|_{t=t^-} > 0, (\frac{dy}{dt})\Big|_{t=t^-} < 0 \Rightarrow (\frac{dx}{dt})\Big|_{t=t^+} = -k$$

$$c: (\frac{dx}{dt})\Big|_{t=t^-} < 0, (\frac{dy}{dt})\Big|_{t=t^-} > 0 \Rightarrow (\frac{dx}{dt})\Big|_{t=t^+} = -k$$

$$d: (\frac{dx}{dt})\Big|_{t=t^-} < 0, (\frac{dy}{dt})\Big|_{t=t^-} < 0 \Rightarrow (\frac{dx}{dt})\Big|_{t=t^+} = k$$

where

$$\frac{dy}{dx} = (dy/dt) / (dx/dt)$$

The above four cases can be expressed as the follows:

$$\text{if} \quad (\frac{dy}{dx})\Big|_{t=t^-} > 0 \quad \text{then} \quad (\frac{dx}{dt})\Big|_{t=t^+} = k \tag{4}$$

$$\text{if} \quad (\frac{dy}{dx})\Big|_{t=t^-} < 0 \quad \text{then} \quad (\frac{dx}{dt})\Big|_{t=t^+} = -k \tag{5}$$

From the above equations, it can be obtained that:

$$\frac{dx}{dt} = K \cdot sign(\frac{dy}{dx}) \tag{6}$$

Presented in Figure 6 is an output curve of a solar cell with the four points a, b, c, d, in which the measurement of the algorithm is determined by dx/dt, while the dynamics is by dy/dx. It is noted from Equation (6) that the balance point $dy/dx = 0$ corresponds to the extremum point of the *y versus x* curve in Figure 5, and the system dynamics are dependent on the slope of such curve. In order to prove the stability at such balance point, a Lyapunov function is selected as:

$$V_{Ly}(t) = \frac{1}{2}(\frac{dy}{dx})^2 \tag{7}$$

The first time derivative of Equation (7) yields:

$$\dot{V}_{Ly}(t) = \frac{dy}{dx}\frac{d^2y}{dx^2}\frac{dx}{dt} = \frac{dy}{dx}\frac{d^2y}{dx^2}(K \cdot sign(\frac{dy}{dx})) \tag{8}$$

It is gained from Figure 6 that:

$$\frac{d^2y}{dx^2} < 0 \tag{9}$$

$$\frac{dy}{dx} sign(\frac{dy}{dx}) > 0 \tag{10}$$

hence, a choice of positive K satisfies $\dot{V}_{Ly}(t) < 0$, *i.e.*, a validated stability.

Relative to conventional MPPT approaches, the adoption of ESC achieves a faster response [11], and then the task of a MPPT controller is completed in this work.

Figure 6. An illustration of ESC dynamics.

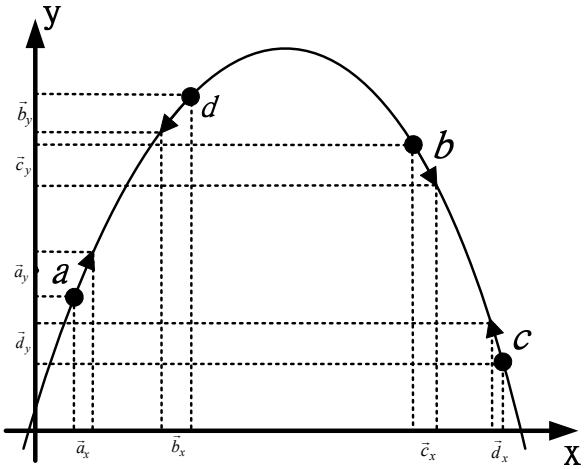

4. Configuration

Illustrated in Figure 7 is a system configuration of this work, in which a PV array is treated as a simulated solar panel. A MOSFET is driven by a PWM sequence generated by ESC to meet the goal of MPPT via a booster with in a simple and easy to implement way.

Figure 7. A system configuration.

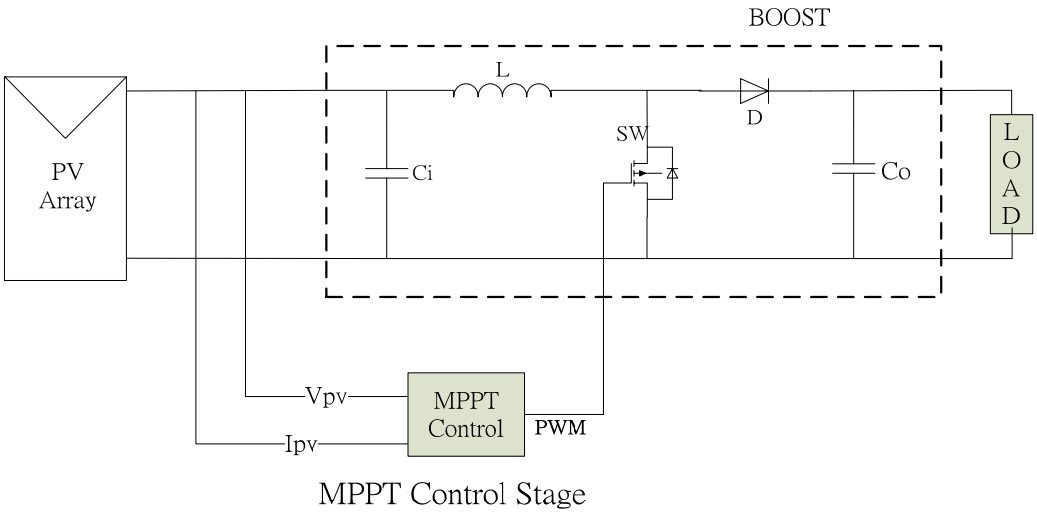

Essentially, the MPPT is the optimization of the solar panel output power. The output power is evaluated as $P_{PV}(t) = V_{PV}(t) * I_{PV}(t)$ by the MPPT controller such that the solar panel is operated at the MPP. Subsequently, the comparison between $P_{PV}(t)$ and $P_{PV}(t-1)$ is made in determination of the output power toward the next instant, *i.e.*, either remaining unchanged or changed. The MOSFET, as referred to previously, is then driven by a PWM sequence, that is, the comparison result between the voltage level at this instant and a triangular waveform. Detailed comparisons are made as follows among the conventional, the sinusoidal and the sliding mode extremum-seeking controls.

4.1. Extremum-Seeking Control

Illustrated in Figure 8 is a block diagram of an ESC system [12]. It shows the simplest way to find the maximum point by ESC method on a *y versus x* curve, *i.e.*, the MPP on the solar cell P-V curve. The current balance point is identified by a gradient detector, subsequent to which modification toward the next instant is determined, and the current signal, stored into memory, is assessed for alteration at the next instant via a switching element. An internal signal is obtained as the multiplication of an integrator gain K by the current signal, and is compared with a triangular waveform to form a PWM sequence so as to drive the MOSFET.

Figure 8. A block diagram of an ESC system.

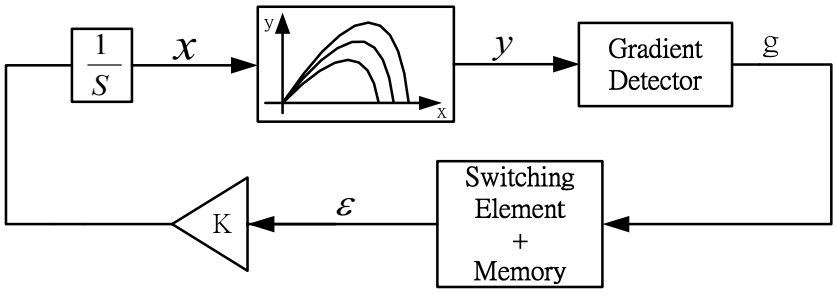

4.2. Sinusoidal Extremum-Seeking Control

Illustrated in Figure 9 [13] is a block diagram of a sinusoidal ESC system, a system applicable to nonlinear control problems. A small amount of perturbation is introduced into a stabilized ESC system, thus affecting the overall system dynamics. Hence, an external sinusoidal disturbance is added to the P-V dynamics in such a way that the MPP can be located as expected via filtered signals. Assuming that there exists an extremum on a concave objective function $y = f(x)$, then the goal of MPPT can be realized with a combination of an integrator, a filter, a multiplier, an adder and a sine wave generator.

Figure 9. A block diagram of a sinusoidal ESC system.

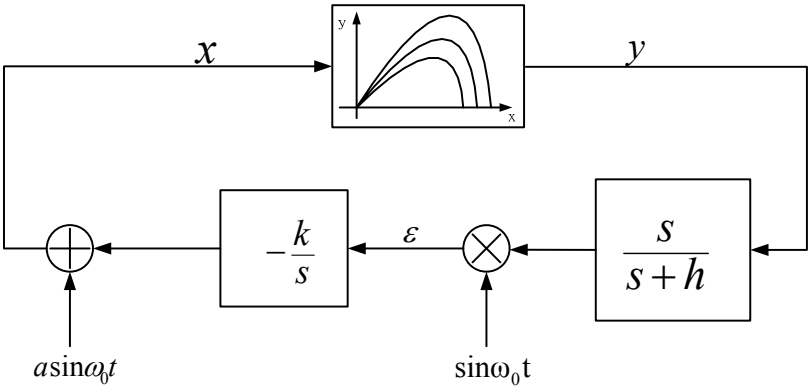

As illustrated in Figure 10, a small amount of sinusoidal perturbation is introduced into the system in the vicinity of MPPT. The perturbation frequency, identical to the central frequency of the filter, must be made lower than that of the triangular wave in the control system. It is noted from Figure 10 that in the case of a negative (positive) ε, the operation point lies on the right (left) of MPPT, respectively. When a small perturbation signal $a \cdot \sin(w_0 t)$, where a denotes the perturbation amplitude and w_0 the frequency w_0, is introduced into the objective function $y = f(x)$, the resultant output is represented as [12]:

$$y = f(x + a \cdot \sin(w_0 t)) \tag{11}$$

Figure 10. An illustration of a sinusoidal perturbation.

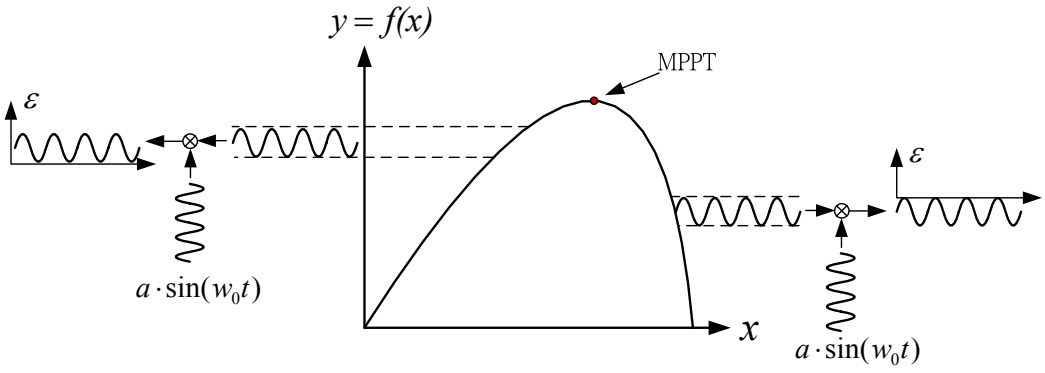

4.3. Sliding Mode Extremum-Seeking Control

Sliding mode control is a kind of non-linear control which is robust in the presence of parameter uncertainties and disturbances [14]. It is able to constrain the system status to follow trajectories which lie on a suitable surface in the sliding surface. The equilibrium state is constructed so that the system restricted to the manifold has a desired behavior. The sliding mode control had been applied to MPPT of solar system by Chu *et al.* [14]. However, the derivation of control law by Chu *et al.* [14] is very complex and it requires an exact system model. This study used the basic sliding mode control law combined with ESC to track the maximum power point in PV system. In comparison with the method of Chu *et al.*, the control law designed by this study is not only easy to implement, but it also does not require the correct model of the system. As illustrated in Figure 11, a sliding mode extremum-seeking control system, unlike the aforementioned two approaches, does not require a gradient detector to determine the signal at the next instant. A disadvantage accompanied by the adoption of such gradient detector is a high frequency switching and damage caused to specific components accordingly, which motivates us to incorporate the idea of sliding mode into ESC to lower down the switching frequency.

A sliding surface is defined as:

$$\sigma = \gamma - y \tag{12}$$

It is known form Figure 11 that:

$$u = dx/dt \tag{13}$$

$$u = U_0 \cdot sign(\sigma) \tag{14}$$

$$dr/dt = \rho + Z \tag{15}$$

$$Z = -Z_0 \cdot sign(\sigma) \tag{16}$$

where U_0 and Z_0 are both constants and the function $sign(\sigma)$ is defined as:

$$sign(\sigma) = \begin{cases} 1 & for\ \sigma > 0, \\ 0 & for\ \sigma = 0 \\ -1 & for\ \sigma < 0 \end{cases}$$

Equation (12) can be rewritten as:

$$\frac{d\sigma}{dt} = \rho - Z_0 \cdot sign(\sigma) - dy/dx \cdot U_0 \cdot sign(\sigma) \tag{17}$$

but the underlying two conditions must be satisfied, *i.e.*,

$$Z_0 >> U_0$$
$$Z_0 >> \rho$$

In order to prove the stability of above SMESC scheme, the Lyapunov function is selected as:

$$V(t) = \frac{1}{2}\sigma^2 \tag{18}$$

Then its first derivative with respect to time is:

$$\begin{aligned}\dot{V}(t) = \sigma\dot{\sigma} &= \sigma[\rho - Z_0 sign(\sigma) - U_0 \frac{dy}{dx} sign(\sigma)] \\ &= \sigma\rho - Z_0|\sigma| - U_0 \frac{dy}{dx}|\sigma| \\ &\le [\rho - Z_0 - U_0 \frac{dy}{dx}]|\sigma|\end{aligned} \tag{19}$$

In the neighborhood of MPPT, the value of $\frac{dy}{dx}$ tends to zero, and it is assumed that $Z_0 >> \rho$ and $Z_0 >> U_0$. Therefore, a chance of suitable positive Z_0 satisfies:

$$\dot{V}(t) < 0 \tag{20}$$

Thus, the stability of this SMESC is proven. A succession of parameter tunings is required to acquire the optimized Z_0 such that the control system is enabled to enter swiftly the sliding surface and reach the robust conditions.

Figure 11. A block diagram of a sliding mode ESC system.

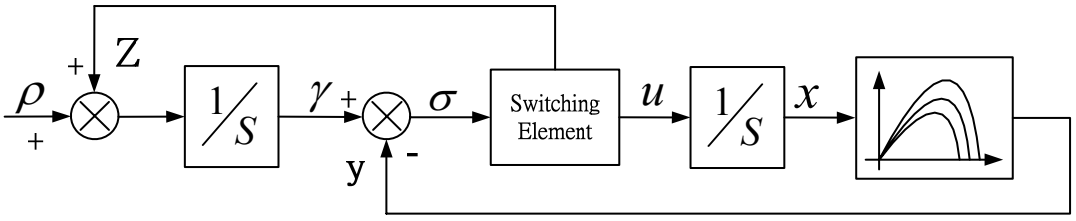

5. Results and Discussion

Tabulated in Table 1 is a data sheet of a KYOCERA KC-KC65T solar panel, which will be simulated with MATLAB subsequently.

Table 1. KC65T data sheet.

$P_{\max}$	V_{MPP}	I_{MPP}	V_{oc}	I_{sc}
65 W	17.4 V	3.75 A	21.7 V	3.99 A

In this work, simulations of all the three extremum-seeking control algorithms are made by MATLAB (sampling time = 0.0001 s) under two conditions, *i.e.*, a uniform irradiance condition and an abrupt one. In the end, the result comparisons are made in respect of overall efficiency and stability.

5.1. Extremum-Seeking Control

Presented in Figure 12 are the conventional ESC time responses under uniform irradiance of 1 kW/m^2 at 25 °C, from which it is noted that there exists large oscillations during the steady and the transient states, respectively. Besides, shown in Figure 13 are the time responses for an abrupt drop in irradiance from 1 kW/m^2 down to 600 W/m^2 at time = 2 s. Even though ESC is still able to accomplish the task of MPPT as shown in Figure 13, there are furious oscillations during rising time and at the

instant the irradiance is suddenly dropped. For this sake, a perturbation signal is introduced in this work to improve the oscillation problem.

Figure 12. Time response of a conventional ESC system under uniform irradiance of 1 kW/m^2 at 25 °C.

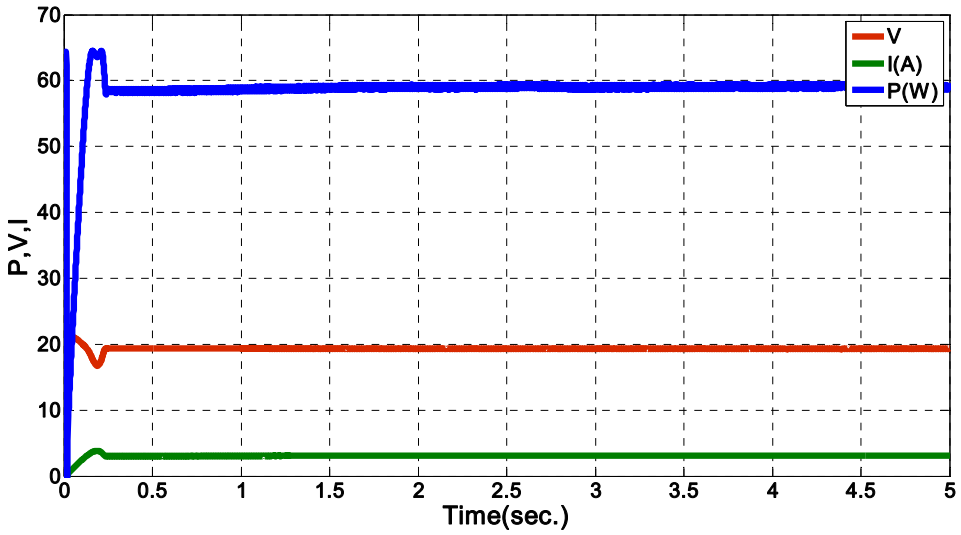

Figure 13. Time response of a conventional ESC system in the context of an abrupt irradiance change from 1 kW/m^2 to 600 W/m^2 at Time = 2 s.

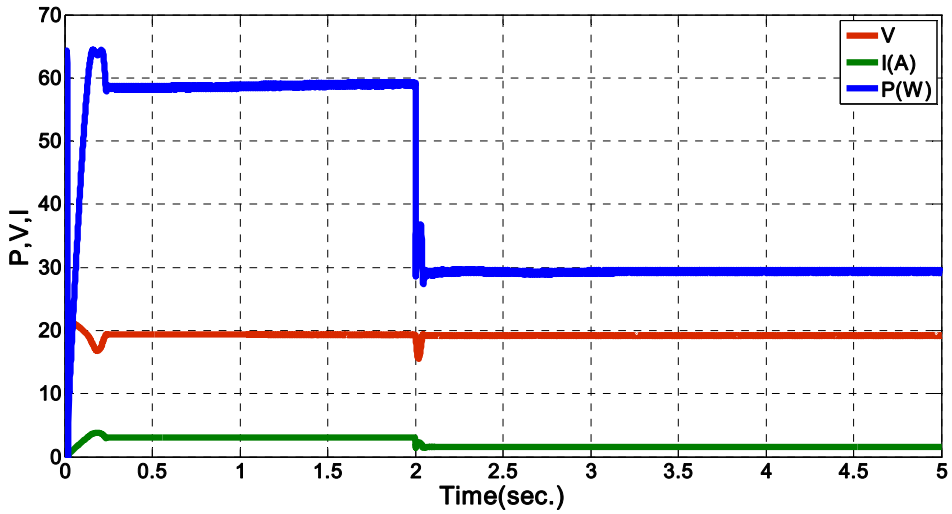

5.2. Sinusoidal Extremum-Seeking Control

Shown in Figure 14 are the time responses of a SinESC system under uniform irradiance of 1 kW/m^2 at 25 °C. It is found that tremendous oscillation of the orginal ESC system is improved by the introduced sinusoidal perturbation and the MPP is precisely tracked as intended. However, the little residual oscillation during the transient state is attributed to the ESC system itself as well as the sinusoidal pertubation. That is, a large oscillation will be seen as a consequence of an increasing amount of simusoidal perturbation, which requies parameter tuning to reduce the steady state oscillation. Presented in Figure 15 are simulations in the case of a drop in irradiance from 1 kW/m^2 to

600 W/m^2 at time = 2 s. Irrespective of the abrupt irradiance change, the MPP can be still precisely tracked as in the previous case, causing an acceptable oscillation in the wake of time = 2 s. It is evident that the SinESC approach does as intended improve the high oscillation suffered in a conventional ESC approach. Plotted in Figures 15 are the voltage and current waveforms of the SinESC system, respectively.

Figure 14. Time response of a SinESC system under uniform irradiance of 1 kW/m^2 at 25 °C.

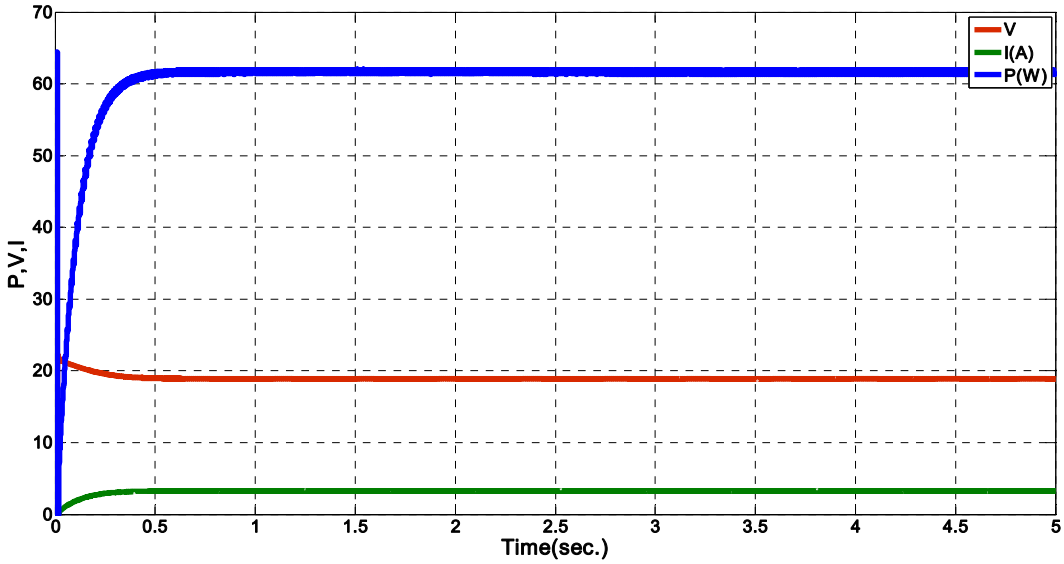

Figure 15. Time response of a SinESC system in the context of an abrupt irradiance change from 1 kW/m^2 to 600 W/m^2 at time = 2 s.

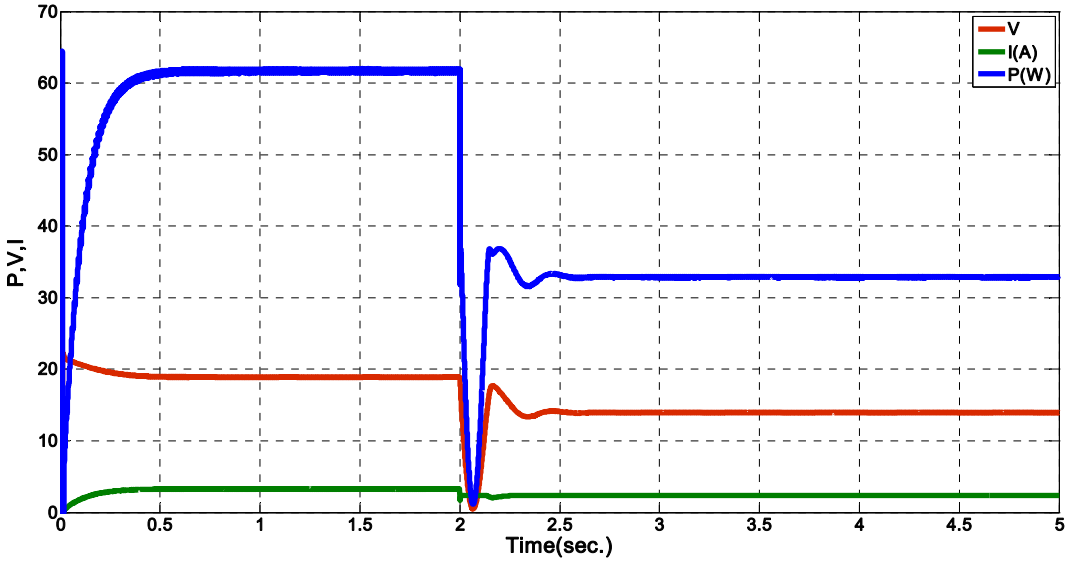

5.3. Sliding Mode Extremum-Seeking Control

Demonstrated in Figure 16 are the output power, voltage and current time responses, respectively, of a SMESC system under uniform irradiance of 1 kW/m^2 at 25 °C. Unlike a conventional ESC or SinESC, there is no need to introduce a sinusoidal perturbation and incorporate a gradient detector, which eliminates a high frequency switching, reduces the power loss and component damage

possibility accordingly. In addition, at time = 2 s, the instant the solar irradiance is suddenly dropped from 1 kW/m^2 to 600 W/m^2, it is found by simulations from Figure 17 that sliding surfaces converge to zero in Figure 17b and successfully track the MPP as intended with a reduced oscillation relative to a conventional ESC system.

Figure 16. Time response of a SMESC system under uniform irradiance of 1 kW/m^2 at 25 °C.

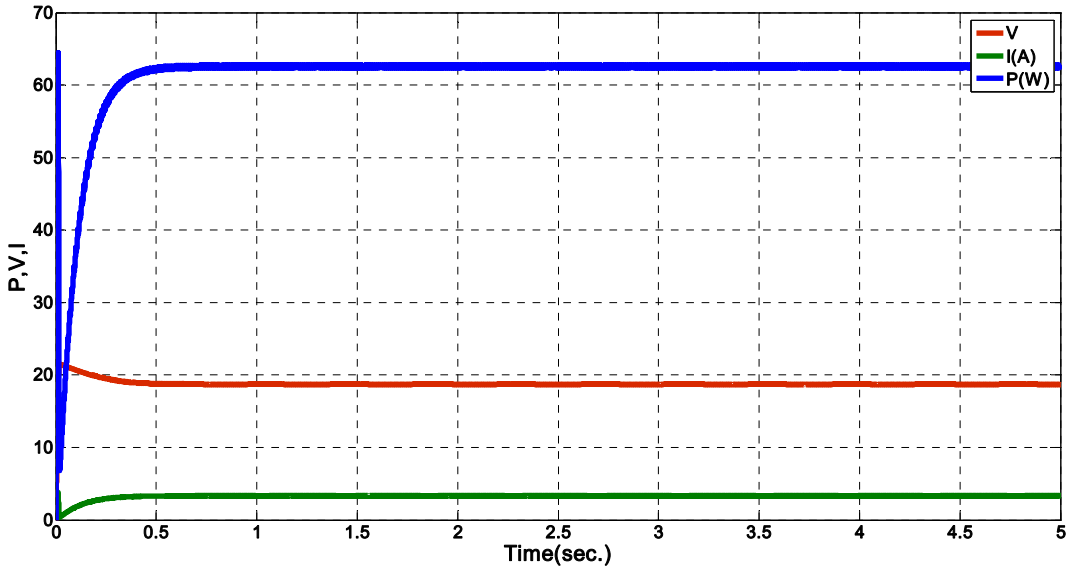

Figure 17. Time response of a SMESC system in the context of an abrupt irradiance change from 1 kW/m^2 to 600 W/m^2 at time = 2 s. (**a**) the output power, voltage and the current waveforms; (**b**) the sliding surface.

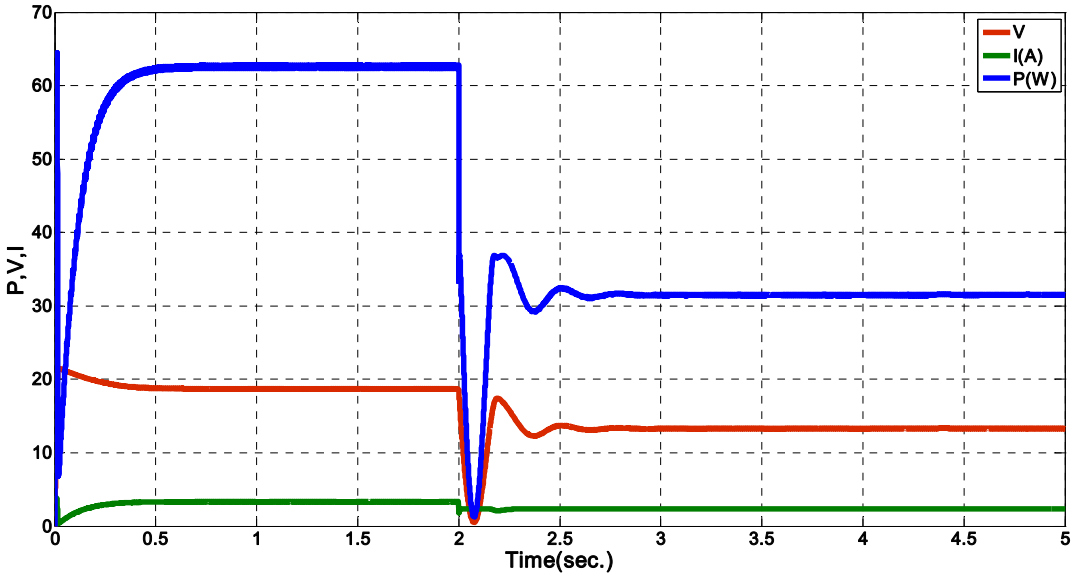

(**a**)

Figure 17. *Cont.*

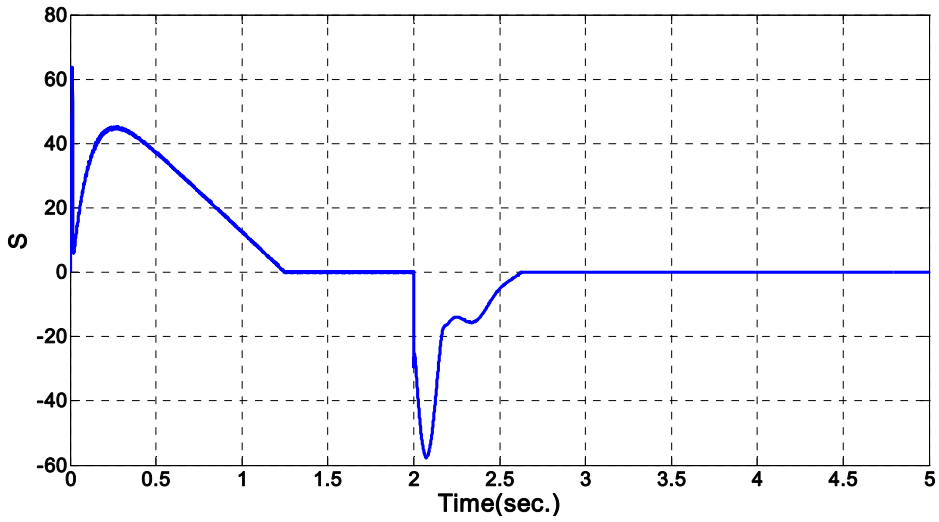

(b)

Plotted in Figure 18 is the output power comparison among ESC, SinESC and SMESC approaches. It is noted that SMESC is the one of the highest output power and ESC is the one of the highest steady state oscillation, not a satisfactory control system on the whole. Yet, although ESC exhibits a shorter rising time, but the SMESC has a smoother response during steady state than ESC, it demonstrates an inferior power output performance than SMESC. Thus, it is demonstrated that SMESC is a better transient response approach than ESC and SinESC, and offers lower steady state oscillation than ESC and SinESC, and the approach in the absence of power loss caused by the high frequency switching as a consequence of a gradient detector employed. In short, the SMESC is an effective algorithm to reach the goal of MPPT.

Figure 18. Output power comparison among ESC, SinESC and SMESC.

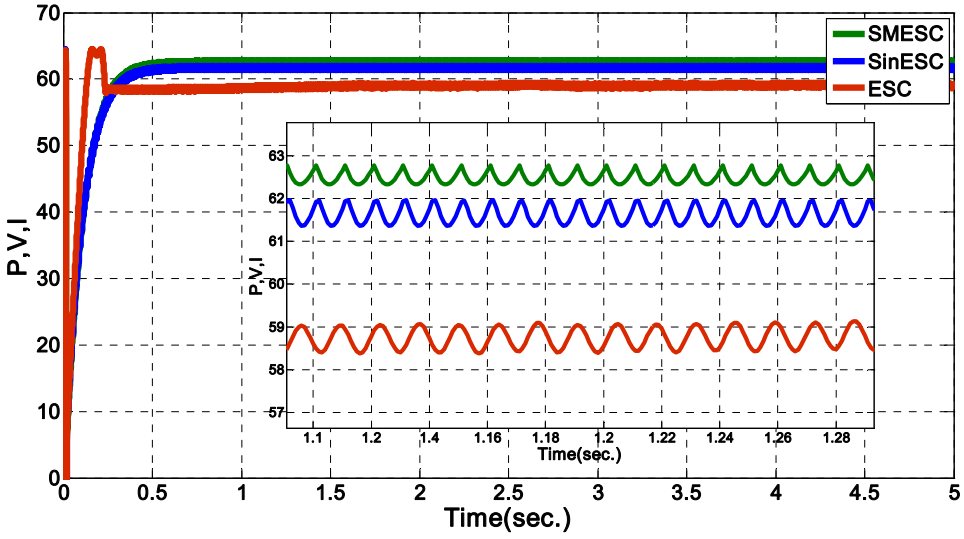

6. Conclusions

A sliding mode extremum-seeking control approach is proposed in this work as a way to carry out the MPPT for a PV system. In comparison with the extremum-seeking control and sinusoidal extremum-seeking control approaches, it is concluded that the SMESC approach is the algorithm with the best overall efficiency. The simulation results show a better transient response than the conventional ESC and SinESC, also a lower steady state oscillation than ESC and SinESC, and the algorithm eliminates the power loss due to the high frequency switching accompanied by a gradient detector. The MPP can be even track in the context of an abrupt change in solar irradiance. Up to now, ESC algorithms have been mostly applied to wind power generation systems, but rarely applied to photovoltaic systems. The sliding mode extremum-seeking control algorithm presented in this work is proven applicable to MPPT tasks for a solar panel.

Acknowledgments

The financial support of this research by the National Science Council of the R.O.C., under Grant No. NSC 100-2628-E-167-002-MY3 is greatly appreciated.

References

1. Krinker, M.; Goykadosh, A. Renewable and Sustainable Energy Replacement Sources. In *Proceedings of the IEEE Applications and Technology Conference (LISAT)*, Farmingdale, NY, USA, 7 May 2010.
2. Kuo, Y.C.; Liang, T.J. Novel maximum-power-point-tracking controller for photovoltaic energy conversion system. *IEEE Trans. Ind. Electron.* **2002**, *48*, 594–601.
3. Liu, F.; Duan, S.F.; Liu, B.; Kang, Y. A variable step size INC MPPT method for PV systems. *IEEE Trans. Ind. Electron.* **2008**, *55*, 2622–2628.
4. Cesare, G.D.; Caputo, D.; Nascetti, A. Maximum power point tracker for portable photovoltaic systems with resistive-like load. *Sol. Energy* **2006**, *80*, 982–988.
5. Wen, F.; Diao, Z.; Chao, Y.; Mo, R. The Design and Implementation of Photovoltaic Grid-connected Simulating Device Based on FPGA. In *Proceedings of the IEEE Power and Energy Engineering Conference*, Chengdu, China, 28–31 March 2010.
6. Benmessaoud, M.T.; Zerhouni, F.Z.; Zegrar, M.; Stambuli, A.B.; Tioursi, M. New approach modeling and a maximum power point tracking method for solar cells. *Comput. Math. Appl.* **2010**, *60*, 1124–1134.
7. Ariyur, K.; Krstic, M. *Real-Time Optimization by Extremum Seeking Control*; Wiley: New York, NY, USA, 2003.
8. Brunton, S.L.; Rowley, C.W.; Kulkarni, S.R.; Clarkson, C. Maximum power point tracking for photovoltaic optimization using ripple-based extremum seeking control. *IEEE Trans. Power Electron.* **2010**, *25*, 2531–2540.
9. Leyva, R.; Alonso, C.; Queinnec, I.; Cid-Pastor, A.; Lagrange, D.; Martinez-Salamero, L. MPPT of photovoltaic system using extremum-seeking control. *IEEE Trans. Aerosp. Electron. Syst.* **2006**, *42*, 249–258.

10. Brunton, S.L.; Rowley, C.W.; Kulkarni, S.R.; Clarkson, C. Maximum Power Point Tracking for Photovoltaic Optimization Using Extremum Seeking. In *Proceedings of the IEEE Photovoltaic Specialists Conference*, Philadelphia, PA, USA, 7–12 June 2009.
11. Cabal, C.; Alonso, C.; Cid-Pastor, A.; Estibals, B.; Seguier, L; Leyva, R.; Schweitz, G.; Alzieu, J. Adaptive Digital MPPT Control for Photovoltaic Applications. In *Proceedings of the IEEE International Symposium on Industrial Electronics*, Vigo, Spain, 4–7 June 2007.
12. Leyva, R.; Artillan, P.; Cabal, C.; Estibals, B.; Alonso, C. Dynamic performance of maximum power point tracking circuits using sinusoidal extremum seeking control for photovoltaic generation. *Int. J. Electron.* **2011**, *98*, 529–542.
13. Olalla, C.; Arteaga, M.I.; Leyva, R.; El Aroudi, A. Analysis and Comparison of Extremum Seeking Control Techniques. In *Proceedings of the IEEE International Symposium on Industrial Electronics*, Vigo, Spain, 4–7 June 2007.
14. Chu C.C.; Chen C.L. Robust maximum power point tracking method for photovoltaic cells: A sliding mode control approach. *Sol. Energy* **2009**, *83*, 1370–1378.